High temperature thermoelectric properties of $Mo_3Sb_{7-x}Te_x$ ($0.0 \leq x \leq 1.8$)

2010 J. Phys.: Condens. Matter 22 025801

(http://iopscience.iop.org/0953-8984/22/2/025801)

J. Phys.: Condens. Matter **22** (2010) 025801 (6pp) doi:10.1088/0953-8984/22/2/025801

High temperature thermoelectric properties of $Mo_3Sb_{7-x}Te_x$ ($0.0 \leqslant x \leqslant 1.8$)

C Candolfi[1,3], B Lenoir[1], C Chubilleau[1], A Dauscher[1] and E Guilmeau[2]

[1] Institut Jean Lamour, UMR CNRS—Nancy Université—UPVM 7198, Ecole Nationale Supérieure des Mines de Nancy, Parc de Saurupt, 54042 Nancy Cedex, France
[2] CRISMAT-ENSICAEN, CNRS/UMR 6508, 6 Boulevard Maréchal Juin, 14050, Caen Cedex, France

E-mail: christophe.candolfi@mines.inpl-nancy.fr and christophe.candolfi@cpfs.mpg.de

Received 13 July 2009, in final form 18 November 2009
Published 14 December 2009
Online at stacks.iop.org/JPhysCM/22/025801

Abstract

Polycrystalline $Mo_3Sb_{7-x}Te_x$ samples with nominal Te concentrations of $x = 0.0$, 0.3, 1.0, 1.6 and 2.2 have been synthesized by a powder metallurgical route. High temperature thermoelectric properties measurements including thermopower (300–900 K), electrical resistivity (300–800 K) and thermal conductivity (300–1000 K) were carried out. The temperature and compositional variations of the thermopower can be satisfactorily explained by assuming a single parabolic band model with dominant acoustic phonon scattering. However, such a simple model fails to describe the electronic thermal conductivity for low Te concentration. The dimensionless figure of merit, ZT, increases on increasing both the temperature and the Te content to reach a maximum value of 0.3 at 800 K that can be extrapolated to ~ 0.6 at 1000 K for $Mo_3Sb_{5.4}Te_{1.6}$.

(Some figures in this article are in colour only in the electronic version)

1. Introduction

The ability of a material to make direct conversion between electrical and thermal energies with high efficiency is typified by the dimensionless thermoelectric figure of merit, ZT, defined as $ZT = \alpha^2 T/\rho\lambda_T = PT/\lambda_T$ [1]. In this formula, α stands for the Seebeck coefficient or thermopower, ρ the electrical resistivity, λ_T the total thermal conductivity, which is the sum of an electronic (λ_e) and a lattice (λ_l) contribution in non-magnetic materials, T the absolute temperature and $P = \alpha^2/\rho$ the power factor.

Intermetallic Zintl phases are currently the focus of great attention due to their potential for thermoelectric applications [2]. These compounds combine the requirements of both good electrical and thermal transport properties to achieve superior thermoelectric properties. Besides having the complex crystalline structures required to attain low thermal conductivities, they offer opportunities to finely tune the electrical properties, through judicious substitutions, with the aim of reaching heavily doped semiconducting behaviour combining high effective masses and high charge carrier mobility.

Among the different families of compounds investigated so far [3–7], $Yb_{14}MnSb_{11}$ and its derivatives were found to definitively demonstrate the thermoelectric potential of this class of materials. While the above-mentioned ternary alloy possesses high ZT values at high temperature ($ZT \sim 1$ at 1275 K), a further improvement has been achieved by substitutions on either the Yb or Mn site by La and Zn or Al, respectively ($ZT \sim 1.3$ at 1223 K in $Yb_{14}Mn_{0.2}Al_{0.8}Sb_{11}$) [8–11].

Recently, another family of compounds classified as a Zintl phase and crystallizing in the cubic Ir_3Ge_7 type structure (space group $Im3m$, 40 atoms per unit cell), namely Mo_3Sb_7 and Re_3As_7, has appeared as promising candidates for power

[3] Author to whom any correspondence should be addressed. Present address: Max-Planck-Institut für Chemische Physik fester Stoffe, Nöthnitzer Straße 40, 01187 Dresden, Germany.

generation [2, 12, 13]. The metallic properties exhibited by these two binary compounds prevent them achieving outstanding thermoelectric properties and they require further optimization [13–15]. By considering the valence of both compounds, they can be rationalized as being two electrons and one hole short of the valence balance, respectively [2]. Therefore, substitutions on the transition metal or metalloid site to add two electrons and one hole, respectively, could drive both systems into a semiconducting state, i.e. to the valence balance. These theoretical assumptions have been experimentally investigated by substituting Ru for Mo, Te for Sb and Ge for As [12, 13, 16–18]. Unfortunately, the solubility limits reached in the $Mo_3Sb_{7-x}Te_x$ and $Mo_{3-x}Ru_xSb_7$ systems ($x \sim 1.6$ for Te and $x \sim 0.8$ for Ru) are lower than the theoretical values required to achieve semiconducting properties ($x = 2.0$ and $x = 1.0$ for Te and Ru, respectively) [12, 16–18]. Nevertheless, these two types of partial substitution have resulted in a significant improvement of the ZT factor, with maximum values of ∼0.8 at 1050 K and ∼0.4 at 1000 K, respectively [12, 16]. Such an enhancement is intimately related to the rigid-like behaviour of the electronic structure when the Te and Ru content increase, as suggested by KKR-CPA calculations [17, 18].

The low temperature transport properties measurements on polycrystalline $Mo_3Sb_{7-x}Te_x$ samples not only confirmed the rigid-band picture but they also shed light on the microscopic mechanisms governing the electrical and thermal conduction processes, as well as on the influence of the exotic magnetic interactions displayed by Mo_3Sb_7 [14]. These interactions arise from antiferromagnetically coupled molybdenum dimers that lead to a spin gap formation at $T^* = 53$ K breaking the cubic symmetry of the crystalline lattice [19–21]. This study has provided compelling experimental evidence of a progressive disappearance of these interactions as the Te content increases. If their influence on the thermopower is rather elusive, the temperature dependences of the electrical resistivity and the thermal conductivity strongly reflect a complex interplay between this low dimensional magnetism and phonon or charge carrier subsystems [14, 18]. Specifically, a crossover from an exotic to a conventional temperature dependence of the thermal conductivity occurs on increasing the Te content [18]. Similar conclusions could be drawn for the $Mo_{3-x}Ru_xSb_7$ compounds [16]. The variations of the thermal conductivity with the Ru content were found to be consistent with the aforementioned picture: phonon–dimer interactions drastically affect the thermal conduction in $Mo_{3-x}Ru_xSb_7$ for low Ru concentrations whereas a conventional temperature dependence is recovered with high Ru content [16].

Since high temperature data have only been collected in the literature for high Te contents ($x = 1.5$ and 1.6) [12], to extend transport properties measurements at high temperature for lower Te concentration may provide additional information regarding the influence of the magnetic interactions. To carry out these investigations, polycrystalline samples of $Mo_3Sb_{7-x}Te_x$ with $x = 0.0, 0.3, 1.0, 1.6$ and 2.2 have been synthesized by a powder metallurgical route. Thermoelectric properties, including electrical resistivity, thermopower and thermal conductivity, have been measured in the 300–800 K, 300–900 K and 300–1000 K temperature range, respectively.

Table 1. EPMA results and relative density (d) of the $Mo_3Sb_{7-x}Te_x$ compounds.

Nominal composition	EPMA	d (%)
Mo_3Sb_7	$Mo_3Sb_{6.95}$	93
$Mo_3Sb_{6.7}Te_{0.3}$	$Mo_3Sb_{6.7}Te_{0.3}$	95
Mo_3Sb_6Te	Mo_3Sb_6Te	96
$Mo_3Sb_{5.4}Te_{1.6}$	$Mo_3Sb_{5.4}Te_{1.6}$	90
$Mo_3Sb_{4.8}Te_{2.2}$	$Mo_3Sb_{5.2}Te_{1.8}$	97

2. Experiment

The synthesis of polycrystalline $Mo_3Sb_{7-x}Te_x$ samples with nominal compositions of $x = 0.0, 0.3, 1.0, 1.6$ and 2.2 was performed by a solid-state reaction method. Stoichiometric quantities of high purity Mo powder (99.999%, Cerac), Sb powder (99.999%, 5N+) and Te powder (99.999%, 5N+) were loaded into a quartz ampoule and sealed under a reducing He–H_2 atmosphere. The ampoules were then heated in a programmable furnace up to 750 °C and kept at this temperature for 15 days. To ensure a good homogeneity of the samples, the obtained ingots were ground in an agate mortar and the powders (∼100 μm) were cold pressed into pellets and further annealed at 750 °C for 15 days. The densification of the powdered samples was realized by hot pressing in graphite dies using graphite foil under an argon atmosphere at 650 °C for 2 h and under a pressure of 51 MPa. The resulting cylindrical ingots (diameter ∼15 mm) were cut with a diamond wire saw into bar and disk shaped samples, to typical dimensions of $2 \times 2 \times 10$ mm^3 and 10 mm in diameter, respectively, for transport properties measurements.

Structural and chemical characterizations of these samples were carried out through x-ray diffraction (XRD), neutron diffraction and by electron probe microanalysis (EPMA) [18, 22]. All the compositions reported in this paper refer to the actual composition inferred from EPMA and normalized to full occupancy of the molybdenum site. It must be emphasized that all the samples studied here are the same as those used for low temperature transport properties investigations [18]. Table 1 summarizes the actual compositions and the relative densities, defined as the ratio of the experimental density to the theoretical density, of the five samples studied.

As previously discussed [18], the $x = 0.0, 0.3, 1.0$ and 1.6 samples are homogeneous and display actual compositions close to the nominal compositions. However, these experiments have unambiguously shown the existence of a solubility limit for Te in Mo_3Sb_7, revealed by the presence of secondary phases in the $x = 2.2$ sample, the actual composition of which was found to be close to $x = 1.8$, in good agreement with that found by Gascoin *et al* [12].

Electrical resistivity measurements were performed in the 300–800 K temperature range by a four probe technique based on the Van der Pauw method. Thermopower measurements were carried out from 300 up to 900 K by a standard method using a commercial system (ZEM 3, Ulvac). The thermal

conductivity was determined in the 300–1000 K temperature range by measuring the thermal diffusivity, a, using a laser flash technique. The thermal conductivity is then obtained using the simple relation $\lambda_T = aC_p\rho$, where C_p and α_T are the specific heat and the volumic mass, respectively. Low temperature measurements have shown that the specific heat values are very close to that expected from the Dulong–Petit law near room temperature. Therefore, the specific heat of all the samples was kept constant to this value throughout the high temperature range investigated. No corrections for thermal expansion at high temperature were applied. Whatever the transport measurement is, a good agreement at room temperature between the low and high temperature values was observed. The deviation is less than 7% for the electrical properties (electrical resistivity and thermopower) and does not exceed 15% for the thermal conductivity.

3. Results and discussion

The temperature dependence of the total thermal conductivity is shown in figure 1(a). While for $x = 0.0$, 0.3 and 1.0 the total thermal conductivity increases with increasing temperature, a very different picture arises for higher Te concentration ($x = 1.6$ and 1.8) since a decrease of λ_T with increasing temperature occurs. This behaviour with regard to the Te content appears similar to that reported in the $Mo_{3-x}Ru_xSb_7$ compounds [16]. Interestingly, in the range of temperature investigated, the thermal conductivity values decrease with increasing Te content, whereas the opposite trend has been clearly observed at low temperature [18]. The decrease of λ_T in the whole temperature range for $x = 1.6$ and 1.8 further reveals the absence of a bipolar contribution up to 1000 K.

To go further, we tried to separate the lattice and electronic contributions from the total thermal conductivity for the five samples studied. However, at high temperature, the Lorenz number can no longer be assumed to be equal to the value of a fully degenerate electron gas, L_0, since this hypothesis would lead to an electronic contribution equal or even higher than the total thermal conductivity for $T > 300$ K for the $x = 0.0$, 0.3 and 1.0 samples. Galvanomagnetic experiments performed at low temperatures have shown that acoustic phonons are the most prominent scatterers of the charge carriers in the $x = 1.6$ and 1.8 samples above 100 K [18]. It is therefore reasonable to assume, as a starting point, that this scattering mechanism is equally at play at high temperature in these compounds. If we further assume that this mechanism also dominates for lower Te concentration, we can then estimate the Lorenz number, L, using the formalism derived from the Boltzmann equation within a single parabolic band model

$$L = \left(\frac{k_B}{e}\right)^2 \left\{ \frac{\left(s+\frac{7}{2}\right) F_{s+\frac{5}{2}}(\eta)}{\left(s+\frac{3}{2}\right) F_{s+\frac{1}{2}}(\eta)} - \left[\frac{\left(s+\frac{5}{2}\right) F_{s+\frac{3}{2}}(\eta)}{\left(s+\frac{3}{2}\right) F_{s+\frac{1}{2}}(\eta)} \right]^2 \right\}, \quad (1)$$

where k_B is the Boltzmann constant, e is the elementary charge, s is a parameter reflecting the dominant scattering mechanism of the charge carriers ($-1/2$ for acoustic phonon scattering), η is the reduced Fermi energy and F_i is the Fermi integral of order i. Using the experimental values of the thermopower (see the next paragraphs), this last parameter can be estimated from the expression

$$\alpha = -\frac{k_B}{e}\left(\frac{2F_1(\eta)}{F_0(\eta)} - \eta\right). \quad (2)$$

Equation (2) also enables the determination of the effective mass of the charge carriers, m^*, via the relation

$$p = \frac{4}{\sqrt{\pi}}\left(\frac{2\pi m^* k_B T}{h^2}\right)^{\frac{3}{2}} F_{\frac{1}{2}}(\eta), \quad (3)$$

where h is the Planck constant. The effective mass, the reduced Fermi level and the Lorenz number calculated at 900 K are

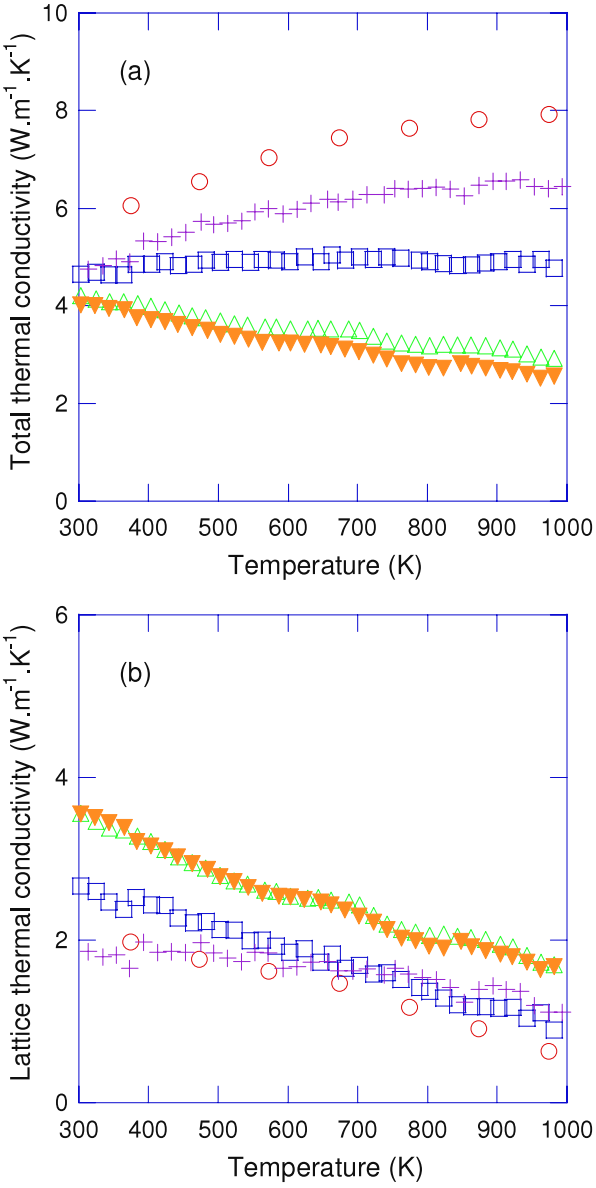

Figure 1. (a) Temperature dependence of the total thermal conductivity of the $Mo_3Sb_{7-x}Te_x$ samples for $x = 0$ (○), $x = 0.3$ (+), $x = 1$ (□), $x = 1.6$ (△) and $x = 1.8$ (▼). (b) Temperature dependence of the lattice thermal conductivity of the $x = 0$ (○), $x = 0.3$ (+), $x = 1$ (□), $x = 1.6$ (△) and $x = 1.8$ (▼) samples.

Table 2. Effective masses (m^*/m_0), reduced Fermi level (η) and Lorenz number (L) estimated from equations (1)–(3) at 900 K. For comparison, the Lorenz numbers estimated at 300 K have been added.

Chemical formula	$m*/m_0$	η	$L_{300\ K}$ ($\times 10^{-8}$ V^2 K^{-2})	$L_{900\ K}$ ($\times 10^{-8}$ V^2 K^{-2})
Mo_3Sb_7	3.8	5.0	2.40	2.18
$Mo_3Sb_{6.7}Te_{0.3}$	4.6	4.1	2.39	2.11
Mo_3Sb_6Te	4.7	2.6	2.33	1.93
$Mo_3Sb_{5.4}Te_{1.6}$	5.0	1.7	2.23	1.82
$Mo_3Sb_{5.2}Te_{1.8}$	4.5	1.2	2.15	1.75

listed in table 2. As can be observed, the effective mass remains relatively unchanged across the entire Te concentration range and the L values show some deviations from L_0 at high temperature for $x = 1.6$ (10%) and $x = 1.8$ (15%), suggesting a lower degree of degeneracy in these two samples.

As a rough approximation, the calculated Lorenz numbers can be used to estimate the electronic thermal conductivity in the whole temperature range investigated via the Wiedemann–Franz law

$$\lambda_e = \frac{LT}{\rho}. \quad (4)$$

The temperature dependence of the lattice thermal conductivity, obtained by subtracting the electronic thermal conductivity from the total thermal conductivity, is shown in figure 1(b). At 1000 K, the λ_l values range between 0.6 and 1.8 W m^{-1} K^{-1}. While the $x = 1.6$ and 1.8 samples display similar lattice contributions, the lattice thermal conductivity of the $x = 0.0, 0.3$ and 1.0 samples is significantly lower. This result is really surprising since, *a priori*, a decrease of the lattice thermal conductivity with increasing disorder is expected even though mass fluctuation effects should be small in the present case (Sb and Te exhibit similar atomic radii and molar masses). The relative densities of the samples cannot solely explain such a difference. Assuming a constant lattice contribution of ~1.8 W m^{-1} K^{-1} at 1000 K across the entire Te concentration range would lead to a Lorenz number value of ~0.6×10^{-8} V^2 K^{-2} for Mo_3Sb_7. This value is much lower than that calculated within a single parabolic band model with electronic properties dominated by acoustic phonon scattering. Hence, this result provokes several comments. The first is that the hypothesis of either a single parabolic band or a single scattering mechanism may fail at low Te concentration. Alternatively, since a progressive disappearance of the magnetic interactions as the Te content increases was highlighted by low temperature magnetic susceptibility together with transport properties measurements [18], one may therefore question whether there is a possible role of these interactions, as an additional scattering mechanism, either on the electronic and/or lattice thermal conductivity of this intriguing system. Actually, rather than speculating about the actual value of the Lorenz number, these unusual results raise the question whether or not these magnetic interactions do play a crucial role on the lattice thermal conductivity of these materials at low substitution levels.

Figure 2 shows the temperature dependence of the thermopower of the five compounds studied. Whatever the sample is, the Seebeck coefficient is positive, indicative of hole conduction. A metallic or highly degenerate behaviour is observed, typified by a linear increase of α with temperature. Since Te atoms provide electrons to the structure, increasing x results in a decrease of the hole concentration and thus, in an increase of the thermopower as can be seen in figure 2. The highest values attained in the temperature range investigated for $x = 1.6$ and 1.8 are similar to those measured in $Mo_{3-x}Ru_xSb_7$ and in excellent agreement with those reported by Gascoin *et al* for a Te content of $x = 1.5$ and 1.6 [12, 16]. Moreover, no maximum in the whole temperature range can be observed, suggesting that the $x = 1.6$ and 1.8 samples do not experience minority carrier effects, as already revealed by the thermal conductivity measurements.

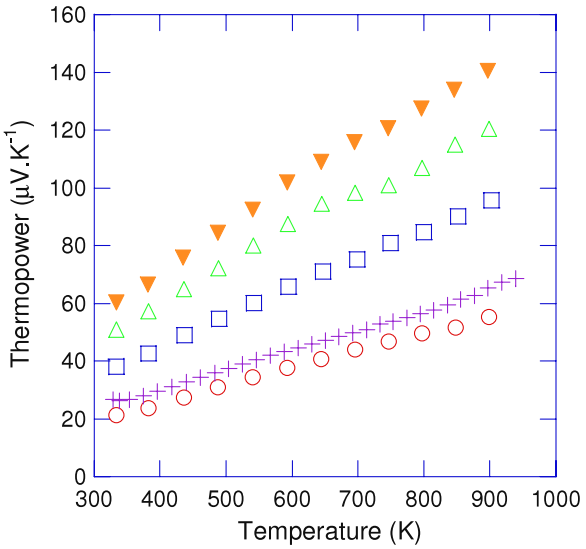

Figure 2. Thermopower as a function of the temperature of the $Mo_3Sb_{7-x}Te_x$ compounds for $x = 0$ (○), $x = 0.3$ (+), $x = 1$ (□), $x = 1.6$ (△) and $x = 1.8$ (▼).

Note that the experimental carrier concentration dependence of the thermopower can be satisfactorily fitted at 300, 700 and 900 K using equations (2) and (3) and an average effective mass $m^* \sim 4.3m_0$, as shown in figure 3. These results seem to support a rigid-band scenario with dominant hole–acoustic phonon scattering even at low Te content.

Figure 4 illustrates the temperature dependence of the electrical resistivity which rises with temperature for the five samples studied. As expected from a rigid-like behaviour of the electronic structure [18], the electrical resistivity increases with the Te content. In the present case, the measured values of the $x = 1.6$ compound are higher than those reported by Gascoin *et al* for the same Te content [12]. However, the lower relative density of our sample mainly accounts for this slight discrepancy.

As figure 5 attests to, the increase of the Seebeck coefficient, together with the decrease of the total thermal conductivity with the Te content, lead to a strong enhancement of the dimensionless figure of merit ZT. Within the temperature range investigated, the ZT values increase with increasing temperature. A maximum ZT value of 0.3 is achieved at 800 K and can be extrapolated to ~0.6 at 1000 K

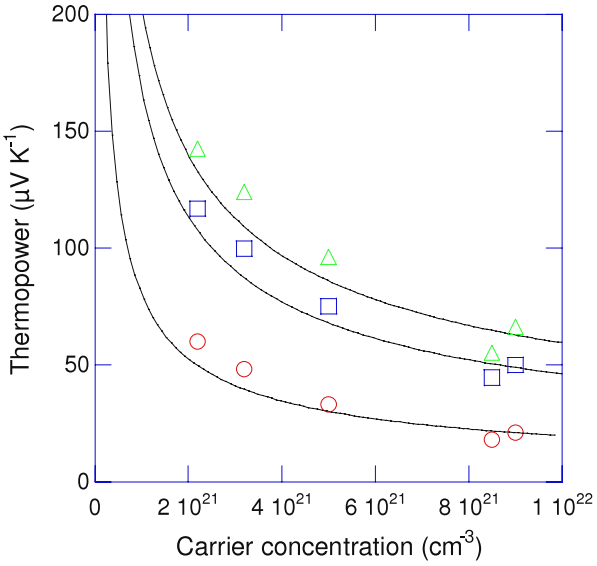

Figure 3. Thermopower as a function of the hole concentration, p, at 300 K (○), 700 K (□) and 900 K (△). The solid lines stand for the best fit to the data according to relations (2) and (3).

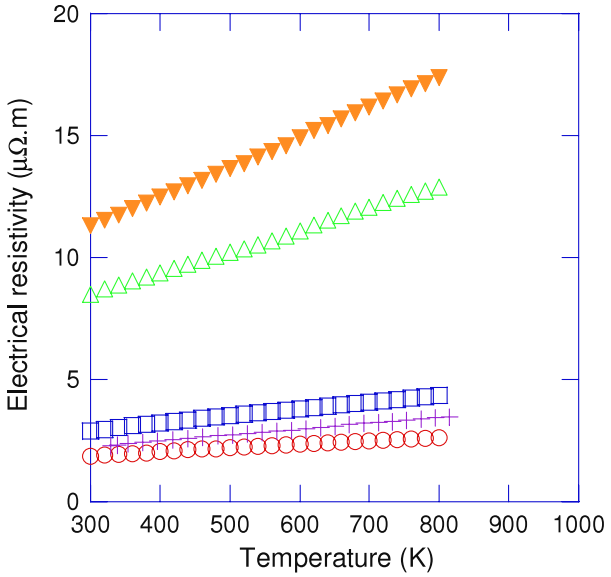

Figure 4. Temperature dependence of the electrical resistivity of the $Mo_3Sb_{7-x}Te_x$ samples for $x = 0$ (○), $x = 0.3$ (+), $x = 1$ (□), $x = 1.6$ (△) and $x = 1.8$ (▼).

for the $Mo_3Sb_{5.4}Te_{1.6}$ compound. This value is higher than the maximum value reported in $Mo_{2.2}Ru_{0.8}Sb_7$ ($ZT \sim 0.4$ at 1000 K) [23]. Even though the electrical resistivity values are higher than those reported by Gascoin *et al* [12], this ZT value is consistent with previous results ($ZT \sim 0.7$ at 1000 K for $x = 1.6$). These results also underline the deleterious influence of the presence of secondary phases exhibited by the $x = 1.8$ sample on the thermoelectric properties.

4. Conclusion

Transport properties measurements on polycrystalline $Mo_3Sb_{7-x}Te_x$ samples have demonstrated the beneficial effect of

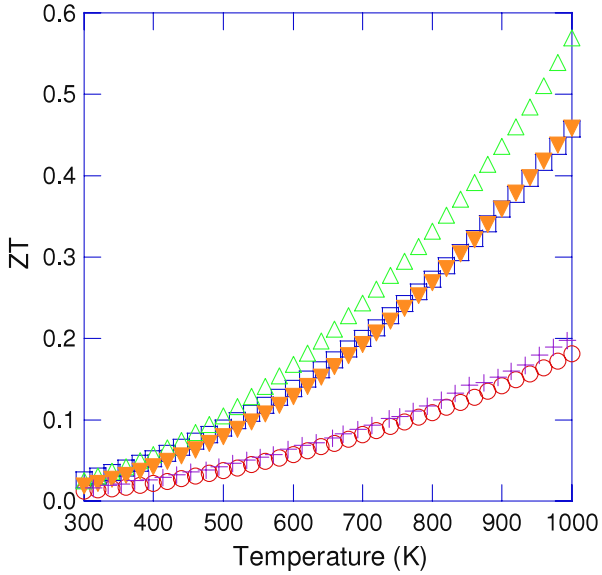

Figure 5. Temperature dependence of the dimensionless figure of merit ZT of the $Mo_3Sb_{7-x}Te_x$ compounds for $x = 0$ (○), $x = 0.3$ (+), $x = 1$ (□), $x = 1.6$ (△) and $x = 1.8$ (▼).

Te on the thermoelectric properties of Mo_3Sb_7. A single parabolic band model, with acoustic phonon scattering as the dominant scattering mechanism of holes, explains the variations against temperature and x of the thermopower in the whole Te concentration range. If this model can be satisfactorily extended to the electronic thermal conductivity for high Te concentration, this simple picture fails to provide a pertinent theoretical background at lower Te concentration. The maximum ZT values reached at high temperature, position these p-type compounds as promising candidates for power generation applications. There is still important phase space to be explored. Alloying with other elements on the Mo and Sb sublattices, as well as studying possible quaternary alloys, may constitute an interesting undertaking to optimize the thermoelectric properties of Mo_3Sb_7.

Acknowledgments

CC greatly thanks M Amiet and P Maigné, and acknowledges the financial support of DGA (Délégation Générale pour l'Armement, Ministry of Defense, France) and the European Network of Excellence CMA (Complex Metallic Alloys).

References

[1] Ioffe A F 1960 *Physics of Semiconductors* (New York: Academic)
[2] Kauzlarich S M, Brown S R and Snyder G J 2007 *Dalton Trans.* 2099–107 and references therein
[3] Gascoin F, Ottensmann S, Stark D, Haile S M and Snyder G J 2005 *Adv. Funct. Mater.* **15** 1860–4
[4] Wang X-J, Tang M-B, Zhao J-T, Chen H-H and Yang X-X 2007 *Appl. Phys. Lett.* **90** 232107
[5] Yu C, Zhu T J, Zhang S N, Zhao X B, He J, Su Z and Tritt T M 2008 *J. Appl. Phys.* **104** 013705
[6] Wang X-J, Tang M-B, Chen H-H, Yang X-X, Zhao J-T, Burkhardt U and Grin Yu 2009 *Appl. Phys. Lett.* **94** 092106

[7] Zhang H, Zhao J-T, Grin Yu, Wang X-J, Tang M-B, Man Z-Y, Chen H-H and Yang X-X 2008 *J. Chem. Phys.* **129** 164713
[8] Brown S R, Kauzlarich S M, Gascoin F and Snyder G J 2006 *Chem. Mater.* **18** 1873–7
[9] Brown S R, Toberer E S, Ikeda T, Cox C A, Gascoin F, Kauzlarich S M and Snyder G J 2008 *Chem. Mater.* **20** 3412–9
[10] Toberer E S, Brown S R, Ikeda T, Kauzlarich S M and Snyder G J 2008 *Appl. Phys. Lett.* **93** 062110
[11] Toberer E S, Cox C A, Brown S R, Ikeda T, May A F, Kauzlarich S M and Snyder G J 2008 *Adv. Funct. Mater.* **18** 2795–800
[12] Gascoin F, Rasmussen J and Snyder G J 2007 *J. Alloys Compounds* **427** 324–9
[13] Soheilnia N, Xu H, Zhang H, Tritt T M, Swainson I and Kleinke H 2007 *Chem. Mater.* **19** 4063–8
[14] Candolfi C, Lenoir B, Dauscher A, Guilmeau E, Tobola J, Wiendlocha B and Kaprzyk S 2009 *Phys. Rev.* B **79** 035114
[15] Candolfi C, Lenoir B, Dauscher A, Bellouard C, Hejtmanek J, Santava E and Tobola J 2007 *Phys. Rev. Lett.* **99** 037006
[16] Candolfi C, Lenoir B, Dauscher A, Hejtmanek J and Tobola J 2009 *Phys. Rev.* B **80** 155127
[17] Candolfi C, Lenoir B, Leszczynski J, Dauscher A, Tobola J, Clarke S J and Smith R I 2009 *Inorg. Chem.* **48** 5216–23
[18] Candolfi C, Lenoir B, Dauscher A, Hejtmanek J and Tobola J 2009 *Phys. Rev.* B **79** 235108
[19] Tran V H, Miiller W and Bukowski Z 2008 *Phys. Rev. Lett.* **100** 137004
[20] Koyama T, Yamashita H, Takahashi Y, Kohara T, Watanabe I, Tabata Y and Nakamura H 2008 *Phys. Rev. Lett.* **101** 126404
[21] Koyama T, Yamashita H, Kohara T, Tabata Y and Nakamura H 2008 *Mater. Res. Bull.* **44** 1132–5
[22] Candolfi C, Lenoir B, Dauscher A, Tobola J, Clarke S J and Smith R I 2008 *Chem. Mater.* **20** 6556–61
[23] Candolfi C, Lenoir B, Leszczynski J, Dauscher A and Guilmeau E 2009 *J. Appl. Phys.* **105** 083701